conservation

Article

Environmental Drivers of Immature Whale Shark Surface Sightings in the Gulf of Tadjoura, Djibouti

Francesca Romana Reinero [1,*], Andrea Marsella [2], Gaetano Vitale [1], Antonio Pacifico [3], Makenna Mahrer [4] and Primo Micarelli [1,5]

[1] Sharks Studies Centre-Scientific Institute, 58024 Massa Marittima, Italy; gaetanovitale16@gmail.com (G.V.); direzione@centrostudisquali.org or primo.micarelli@unisi.it (P.M.)
[2] Istituto Zooprofilattico Sperimentale delle Venezie, 35020 Legnaro, Italy; amarsella@izsvenezie.it
[3] Department of Information Engineering, Computer Science, and Mathematics, University of L'Aquila, 67100 L'Aquila, Italy; antonio.pacifico@univaq.it
[4] W.M. Keck Science Department, Claremont McKenna College, Claremont, CA 91711, USA; mmahrer23@students.claremontmckenna.edu
[5] Department of Physical Sciences, Earth and Environment, University of Siena, 53100 Siena, Italy
* Correspondence: ricerca@centrostudisquali.org

Abstract

Whale sharks seasonally aggregate in Djibouti (East Africa), supporting ecotourism activities which benefit the local community. However, the environmental factors influencing whale shark relative abundance at this site are still not well understood. Environmental drivers of immature whale shark surface sightings have been analyzed across a five-year period (2017, 2020, 2022, 2024 and 2025) in the Gulf of Tadjoura (Djibouti) using a Generalized Additive Model (GAM) and Hurdle model. Across 111 surface sightings and 83 photo-identified whale sharks, both sea surface chlorophyll-*a* (SSC) concentrations and sea surface temperature (SST) have significantly affected their relative abundance ($p < 0.001$), while wind strength appeared to have a weaker and more complex effect ($p < 0.05$). Whale shark surface sightings in the Gulf of Tadjoura increased when SSC and SST exceeded thresholds of 0.5 mg/m^{-3} and 26 °C, respectively. In contrast, the positive effect of wind strength ≥ 7 knots was limited, indicating that wind-driven influences on whale shark surface detections are localized and transient. Since prey abundance and distribution are the main drivers of whale shark seasonal aggregations, understanding the environmental effects on food availability at coastal locations and, consequently, on whale shark surface sightings is crucial. The present study highlights temporal and seasonal trends in whale shark sighting data, contributing to broader initiatives aimed at improving conservation and management strategies for this endangered species.

Keywords: elasmobranch; *Rhincodon typus*; environmental factors; relative abundance; aggregation

Academic Editor: Just Tomàs Bayle-Sempere

Received: 29 September 2025
Revised: 31 October 2025
Accepted: 7 November 2025
Published: 14 November 2025

Citation: Reinero, F.R.; Marsella, A.; Vitale, G.; Pacifico, A.; Mahrer, M.; Micarelli, P. Environmental Drivers of Immature Whale Shark Surface Sightings in the Gulf of Tadjoura, Djibouti. *Conservation* **2025**, *5*, 68. https://doi.org/10.3390/conservation5040068

1. Introduction

Elasmobranchs, particularly sharks, function as top or mesopredators that exert a significant influence on regulating trophic structure and ecological function [1,2]. A decline in local shark populations may induce trophic cascades, altering prey behavior and abundance across marine communities [3–6]. Most studies have focused on shark decline caused by overfishing [7–10]. However, environmental factors are crucial drivers for predicting shark abundance, distribution, and behavior, ultimately shaping community structure and dynamics [11]. Environmental factors may alter sharks' abundance either directly, influencing

key physiological processes such as growth, reproduction, and metabolism and affecting habitat suitability through changes in physical and chemical water parameters [12], or indirectly, altering prey availability and distribution [13].

Abundance is a valuable metric because it can describe population changes and dynamics over space and time [14]. Absolute abundance refers to the total number of individuals in a specific area, providing the most accurate estimate of a true population size [14]. On the contrary, relative abundance serves as a proxy, typically assessing variations in the presence or density of species across temporal and spatial gradients [15]. This distinction is particularly relevant when studying species characterized by extensive movement capabilities like sharks, which perform vertical mobility behavior and spend an unknown portion of time at depth, making their detection through visual or aerial surveys difficult [16–18]. Relative abundance is often misinterpreted as absolute abundance [14], and few studies report shark abundance estimates from surface sightings [19–22]. These may include availability bias, referring to the portion of time during which the animal is present at the surface and available for detection, and perception bias, referring to the possibility of not detecting the animal despite its presence at the surface [23]. Addressing these biases in the analysis offers a robust and replicable framework for future research. Despite their limitations, surface-based surveys remain a valuable tool, particularly for those species inhabiting coastal areas and subjected to high anthropogenic pressure [24,25].

The whale shark (*Rhincodon typus*, Smith 1828) is the largest fish on Earth and a plankton-feeding species. In Djibouti, seasonal aggregations of whale sharks in coastal waters between October and February are driven by increased zooplankton biomass resulting from monsoon seasonal variability [26–31]. In this area, whale shark coastal aggregations predominantly consist of immature males feeding on dense concentrations of zooplanktonic organisms with copepods comprising over 80% of their diet [30,32,33]. This aggregation allows the growth of ecotourism activities and, consequently, the repeated sightings of whale sharks near the surface [30,31].

While whale shark ecology has been widely investigated in Djibouti [26–35], there are still unresolved issues concerning abiotic drivers of whale shark presence and surface sightings [30]. Reinero et al. [31] demonstrated that sea surface chlorophyll-*a* (SSC) concentrations in the Gulf of Tadjoura (Djibouti), influenced in turn by additional environmental variables, serve as predictors of the surface feeding behavior of immature male whale sharks, providing valuable insights into relative abundance and distribution patterns. Despite the limited knowledge regarding the environmental drivers of whale shark relative abundance in Djiboutian waters, several studies investigated their effects in other aggregation sites worldwide [19,36–44].

For instance, a positive correlation between SSC, sea surface temperature (SST) and whale shark surface sightings was observed in Ningaloo Reef, Australia [36]. Likewise, specific ranges of SSC and SST could affect whale shark presence in Cenderawasih Bay, Indonesia [40]. Similar trends were reported in the western Indian Ocean [42] and in the south Ari Atoll in the Maldives [39], where an increase in whale shark abundance was linked to higher SSTs. On the contrary, in the Seychelles, a negative correlation between SST, wind speed, and whale shark surface sightings was highlighted [19]. However, in Mozambique [38] and Kilindoni Bay, Mafia [41], SST did not predict whale shark abundance, and other environmental variables such as wave height [38], bathymetry [43], zooplankton abundance, moon illumination, and weather conditions [41] were identified as more heavily correlated. Other predictors could play a broader role in shaping whale shark abundance, such as El Niño-Southern Oscillation (ENSO). In Ningaloo Reef, Wilson et al. [44] observed a higher number of whale sharks during La Niña events. In the same area, Sleeman et al. [37] suggested that colder ENSO events and stronger along-shelf winds were associated with

higher whale shark abundance, since the intensity of oceanic processes such as Leeuwin Current and wind-driven upwelling may alter the prey availability in the region and, consequently, the number of whale sharks at this site.

Therefore, understanding the relationship between a species and its surrounding environment is crucial, since marine species are often associated with habitats characterized by specific physical and biological conditions [45]. Most observed whale shark aggregations occur in coastal areas worldwide, and identifying environmental drivers of surface sightings could highlight whether observed fluctuations in relative abundance and distribution are due to environmental variability in a climate change scenario or to anthropogenic pressure [38]. Addressing this knowledge gap is particularly important for regions with limited information as Djibouti, in order to develop appropriate conservation strategies for this endangered species and gain new insights into whale shark ecology.

The aims of the present study are to: (i) assess whether whale shark surface sightings in Djibouti are influenced by environmental variables; (ii) identify the primary factors associated with whale shark relative abundance; and (iii) examine the effects of environmental factors on surface sighting patterns.

2. Materials and Methods

2.1. Sampling Area

Sampling was conducted in the coastal waters of Djibouti, within the Gulf of Tadjoura (11°40′ N, 43°00′ E). Fieldwork was carried out aboard the sailing vessel "Elegante" at two whale shark feeding hot spots between Arta Beach (11°58′ N, 42°82′ E) and Ras Korali (11°34′ N, 42°47′ E). Surveys were performed in January 2017, 2020, 2022, 2024, 2025, and November 2022 (Figure 1). Each campaign lasted one week, except for January 2022, which spanned two weeks.

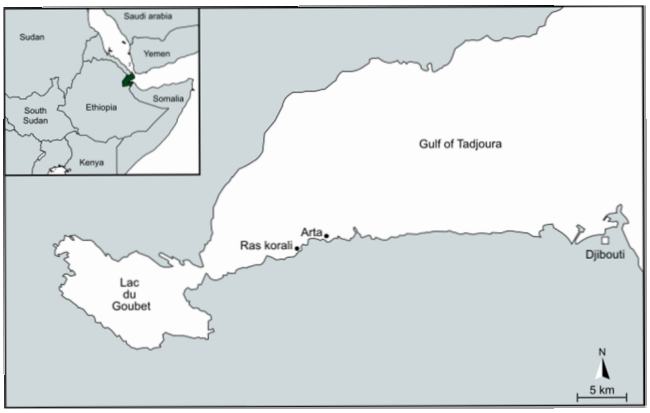

Figure 1. The areas (Arta Beach and Ras Korali) in the Gulf of Tadjoura where sampling activities were performed.

2.2. Whale Shark Surface Sightings

In this study, the sampling areas and methods used to identify individuals and collect environmental variables were the same as those employed by Reinero et al. [31] to assess the environmental drivers of immature whale shark surface feeding behavior.

After anchoring the vessel, two zodiacs were deployed daily between 09:00 and 17:00 h to conduct whale shark sightings. Each zodiac undertook an average of 6 h of surface observations per day over five consecutive days in January 2017, January 2020, November 2022, January 2024, and January 2025, yielding a total of 60 h of observations per year. For the two-week survey in January 2022, the observation time was 120 h. Overall, 420 h of observation time were spent in the Gulf of Tadjoura and sightings occurred within 50 m offshore of both study sites.

Upon sighting an individual, photographs and videos of the right and left sides—dorsally to the pectoral fins and behind the fifth gill slit-were captured using action cameras to facilitate photo-identification. Additional images documented body scars and permanent wound markings [30]. Photo-identification was conducted with the I^3S (Interactive Individual Identification System) Classic software for pattern recognition v4.0 by uploading photographs of specimens to assess potential matches among individuals [29–31,46–48].

Sex determination was performed through direct visual assessment beneath each individual and by visually assessing the presence or absence of claspers in the pelvic region [31]. Initial measurements of individual size were obtained through laser-photogrammetry (from the rostrum to the beginning of the first dorsal fin), and total length (TL) was subsequently estimated following the equation provided by Matsumoto et al. [49]. Size measurements were conducted only during the 2022, 2024, and 2025 campaigns.

Identification sheets were completed for each whale shark, including the number of the identified individual, photographs of right and left sides, observation date and time, observation site, sex (if determined), TL (if determined), photographic and video documentation, and the distribution of injuries and scars. If an individual was re-sighted during the same year or in subsequent survey years, only the first recorded encounter was retained in the identification sheet. However, all re-sightings were documented, along with records of whale shark presence and absence during each sampling period.

2.3. Acquisition of Environmental Variables

Data on environmental variables were recorded in both sampling areas in 2017, 2020, 2022, 2024, and 2025 using a combination of online databases and in situ measurements [31], as follows:

(1) Information on sea conditions was retrieved from the Windguru database https://www.windguru.cz/4910 (accessed on 6 February 2025) for the "Djibouti (East Africa)" region. Conditions were grouped into "calm" (height of waves ranging from 0–10 cm), "slightly rough" (height of waves ranging from 11–50 cm), and "rough" (height of waves exceeding 50 cm).
(2) Information on brightness intensity was retrieved from the number of eighths (oktas) of sky obscured by clouds, following Rees [50]. Oktas were categorized as follows: 0–2 for clear sky; 3–5 for partly cloudy sky; and 6–8 for fully clouded sky.
(3) Information on sea surface temperature (SST), reported in °C, was retrieved from the underwater computer.
(4) Information on wind strength, reported in knots (km/h), was retrieved from the Windguru database for the "Djibouti (East Africa)" region.
(5) Information on rainfall level, reported in mm/h, was also retrieved from the Windguru database for the same region.
(6) Information on sea surface chlorophyll-*a* (SSC) concentration, reported in mg/m^3, was retrieved from the Copernicus Marine Service database https://data.marine.copernicus.eu/ (accessed on 6 February 2025) for both sampling areas.
(7) Information on El Niño Southern Oscillation (ENSO) conditions was expressed using the Multivariate ENSO index (MEI) obtained from the NOAA Climate Prediction Center database https://www.cpc.ncep.noaa.gov/products/analysis_monitoring/enso_advisory/ensodisc.shtml (accessed on 6 February 2025).

2.4. Statistics

To investigate the environmental drivers of whale shark surface sightings across the five-year period, a dataset containing sighting counts and variables representing both indirect and unobserved factors was used. Given the count nature of the response variable

(whale shark surface sightings) and the high frequency of zero sightings, two statistical approaches were employed: a Generalized Additive Model (GAM) aimed to correlate whale shark sightings to environmental drivers, and a Hurdle model to account for zero inflation in the data while modelling shark relative abundance and occurrence.

The explanatory variables consisted of six continuous environmental variables: (i) SST (°C), (ii) SSC (mg/m^3), (iii) brightness intensity (oktas), (iv) wind strength (km/h), (v) rainfall level (mm/h), and (vi) ENSO measurement unit (MEI). Sea condition (vii) was computed based on intensity as an ordinal variable categorised as (1) calm, (2) slightly rough, and (3) rough. The dataset was structured to enhance model fitting and interpretability and to examine the degree of interdependence between indirect and unobserved factors, which represent a potential source of endogeneity. Specifically, environmental continuous variables were discretized and treated as categorical or ordinal indicators: SST (temp) values were categorized as 0 for $\leq$26 °C and 1 for >26 °C; rainfall level (rain) was classified as 0 for 0 mm/h and 1 for >0.0 mm/h; wind strength (wind) was coded as 0 for <7 knots and 1 for $\geq$7 knots; SSC (chl-a) was classified as 0 for $\leq$0.5 mg/m^3 and 1 for >0.5 mg/m^3; and MEI (mei) taking values 0 for <0 and 1 for $\geq$0. The response variable corresponded to the number of whale shark surface sightings recorded during each independent survey effort, treated as a discrete count variable for the three research questions addressed in this study.

Before addressing the three research questions through GAM analysis and the Hurdle model, two non-parametric tests were conducted to assess whether the number of surface sightings influenced by environmental variables differed significantly between months and years.

A Wilcoxon Rank-Sum Test was conducted to examine whether the number of whale shark sightings differed between the two 2022 sampling periods (January and November), with the aim of assessing potential inter-seasonal variation in surface sightings within the same year. The analysis considered two variables: "whale shark surface sightings", treated as a count variable, and "months", treated as an ordinal variable coded as 0 for January and 1 for November. Under the null hypothesis, the number of whale shark surface sightings was assumed independent of the 2022 sampling months, whereas the alternative suggested a dependency between the two variables.

A Kruskal–Wallis test was then performed to explore whether the number of whale shark surface sightings was independent (null hypothesis) or dependent (alternative hypothesis) of the observation years. Notably, the hypothesis testing considered two variables: "whale shark surface sightings" evaluated as a count variable, and "year", as a categorical variable with five different levels (2017, 2020, 2022, 2024, and 2025).

To enhance model robustness and reinforce the assumption of statistical independence, categorical variables were encoded as factors, and the dataset was aggregated by a unique combination of covariates, summing whale shark sightings within each group. This approach was intended to ensure the statistical independence of observations and mitigate data sparsity, thereby facilitating more reliable statistical inferences.

A Generalized Additive Model (GAM) was designed to explore the environmental drivers of whale shark surface sightings. This non-parametric approach enabled a detailed analysis of how these drivers affect surface sightings, revealing the relative contribution of each factor while holding other covariates constant. GAMs extend Generalized Linear Models (GLMs) by replacing strictly linear predictors with additive predictors, allowing us to model non-linear relationships between the explanatory variables (environmental drivers) and the response variable (whale shark surface sightings), as detailed by Equation (1):

$$\log\left(\mathrm{E}[\mathrm{Y}_i]\right) = \beta_0 + f_1(\mathrm{X1}) + f_2(\mathrm{X2}) + \cdots + \quad (1)$$

where Y*i* denotes the response variable for *i*-th observation, E[Y*i*] refers to the expected value (mean) of the response variables for observation *i*, log (·) represents the log link function connecting the linear predictors to the expected value of the response variable, β_0 is the intercept term in the model, and f(X*i*) is a non-parametric function capturing the linear or nonlinear relationship between the predictor variable (X*i*) and the response.

In this study, environmental continuous variables were discretized and treated as categorical or ordinal indicators. While discretization involves certain trade-offs, such as a potential loss of fine-scale information, a moderate capacity to capture complex non-linear relationships and a simplified representation of ecological gradients, it can enhance the interpretability of complex ecological models and remains a common and valid practice in ecological research.

This methodological choice was based on two key considerations: (i) enhancing model interpretability for ecological inference, and (ii) preventing overfitting due to limited unique values in several predictors, making them unsuitable for smooth spline estimation. Independent variables, including 'wind', 'temp', 'chl-a', 'rain', and 'mei', presented a limited number of unique observations ($\leq$4–6 categories), violating the assumptions necessary for thin-plate regression spline estimation within the GAM framework. Attempting to include these predictors as smooth terms resulted in convergence errors and rank deficiencies in spline construction, confirming that a non-parametric treatment was statistically inappropriate for such variables. Consequently, no smooth terms were included in the final GAM specification. All predictors were treated as fixed categorical effects, and the functional form of the GAM was effectively reduced to that of a GLM with categorical covariates. This simplified structure enhanced the model's robustness while retaining the GAM framework's flexibility in handling non-linear effects where applicable.

Prior to model specification, multicollinearity among explanatory variables was assessed using the Generalized Variance Inflation Factor (GVIF) calculated with the car package (v.3.1.3) in the R programming language (v.4.4.3). In this study, each explanatory variable had a $GVIF^{(1/(2*df))} < 5$, indicating an acceptable level of collinearity (Table 1).

Table 1. Generalized Variance Inflation Factors (GVIFs) for predictors included in the initial GAM. "Covariate" refers to environmental factors considered in the study and included in the model. Here, "temp" refers to SST, "wind" refers to wind strength, "chl-a" refers to SSC, "mei" refers to ENSO measurement unit (MEI), "sea" refers to sea condition, "okta" refers to brightness intensity, and "rain" refers to rainfall level; "GVFIs" stand for Generalized Variance Inflation factors, which quantify the inflation in variance due to multicollinearity among predictors; "df" denotes the degree of freedom associated with each variable; and "$GVIFs^{(1/(2*df))}$" describe the adjusted GVIFs providing standardized values to enable comparisons among variables with different degrees of freedom.

Covariate	GVIFs	df	$GVIFs^{(1/(2*df))}$
temp	19.0111	1	4.3602
wind	1.8467	1	1.3589
mei	19.2023	1	4.3820
chl-a	7.1129	1	2.6700
sea	2.4799	2	1.2549
okta	2.0333	1	1.4260
rain	4.4813	1	2.1169

Thus, all the independent variables were included in the initial GAM, as described in Equation (2):

$$\log\left(E[Y_i]\right) = \beta_0 + \beta_1 \cdot SST_i + \beta_2 \cdot chl_i + \beta_3 \cdot Wind_i + \beta_4 \cdot Rain_i + \beta_5 \cdot MEI_i + \beta_6 \cdot SeaCond_i + \beta_7 \cdot okta_i \quad (2)$$

Models were constructed using the mgcv package, specifying a Poisson distribution appropriate for the count data, and a restricted maximum likelihood (REML) method was included to control the overfitting and improve estimation stability. Model selection was performed by comparing the value of explained variance expressed as a percentage (R^2 adjusted) and Akaike's information criterion (AIC). The model explaining the highest variance was chosen since it most accurately captured the variability in the data. Model selection process was conducted using the dredge command from the MuMIn package (v.1.48.11) for R (v.4.4.3).

Given that whale shark sighting rate data collected through visual surveys were zero-inflated, with 54.2% of observations corresponding to non-detections (Figure 2), GAM analysis was combined with the Hurdle model to account for the excess of zeros.

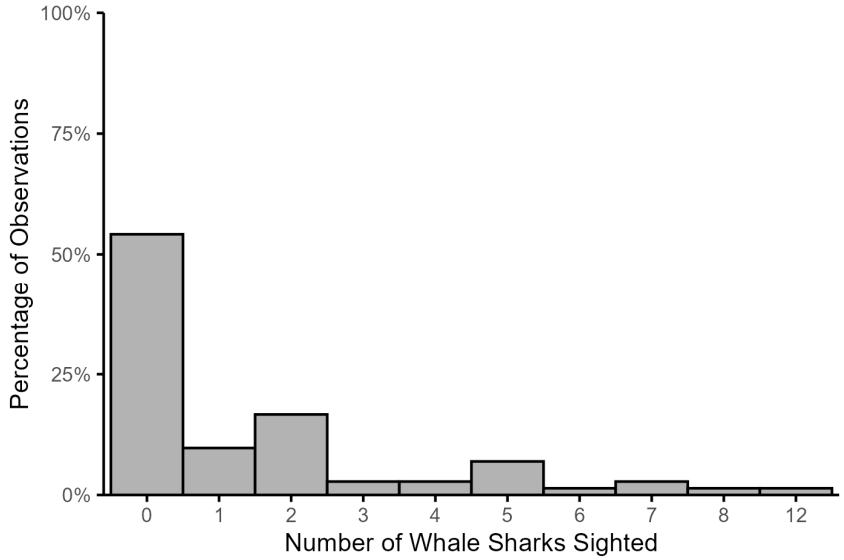

Figure 2. Zero-inflated distribution of whale sharks sighted from visual surveys, with 54.2% of observations corresponding to zero sightings (non-detections), while the remaining observations involved low counts (mostly one or two individuals).

The Hurdle model is divided in two-stage distinct components: (i) the first component includes the zero and non-zero data as binary response (presence/absence) and is modelled by a binomial distribution via linear regression, where zeros are governed by a Bernoulli process; and (ii) the second component (count) contains only the non-zero responses, modelled by a zero-truncated distribution via discrete or continuous GLMs. The general form of a Hurdle model is detailed in Equation (3):

$$\Pr(Y|x,y) = \begin{cases} p(x) & y = 0 \\ 1 - p(x)\frac{f(y)}{1-f(0)} & y > 0 \end{cases} \quad (3)$$

where x denotes a random binary variable, with 0 indicating a negative observation (absence), and 1 denoting a positive observation (presence); and $f(y)$ denotes the probability distribution selected to model the positive observations (≥ 1).

The estimation of parameters in the Hurdle model is conducted separately for each component, enabling independent modelling of the processes influencing surface occurrence and relative abundance. The first component of the model addressed the influence of environmental variables on whale shark surface occurrence, whereas the second component examined their effects on whale shark relative abundance. In this study, a binomial distribution with a logit link to model the whale shark surface presence/absence from all

data was first used. Then, the relative abundance of the sharks using a zero-truncated Poisson distribution with logit link was modelled (Equation (4)):

$$\begin{aligned} \Pr(Y_i = 0) &= 1 - p, \quad 0 \leq p \leq 1, \\ \Pr(Y_i = k) &= p\frac{\mu^k \exp(-\mu)}{k!1-\exp(-\mu)}, \quad k = 1, \ldots, \infty, 0 < \mu < \infty, \end{aligned} \tag{4}$$

where Yi denotes the response variable (whale shark sightings) for i-th observation, μ denotes the mean for an untruncated Poisson distribution, and p denotes the probability of observing a non-zero count.

To determine the most appropriate distribution for the count component of the Hurdle model, a preliminary assessment was conducted comparing two alternative distributions: (i) a truncated Poisson distribution, as data displayed a high frequency of zeros along with right-skewed non-zeros counts indicative of potential zero inflation (Figure 2); (ii) and a truncated negative binomial distribution, which is more effective in accommodating the overdispersion of count data. Subsequently, the best distribution selection was conducted considering two measures of parsimony, AIC and the Bayesian information criterion (BIC), in the R programming language (v.4.4.3). Identifying the best distribution corresponds to choosing the lowest values of AIC and BIC, and the distribution with the best fit was the one used in the final Hurdle model. Subsequently, variable selection was performed, employing a stepwise procedure using AIC. The most parsimonious model for both the zero and count components was selected based on the lowest AIC values. Model fit was subsequently evaluated using McFadden's pseudo-R^2 (Equation (5)):

$$R^2_{MC} = 1 - \frac{\log L_{reduced}}{\log L_{null}} \tag{5}$$

where $\log L_{reduced}$ denotes the log-probability measures from the reduced models (containing the most parsimonious combination of predictors), while $\log L_{null}$ indicates the log-likelihoods of the null model with only an intercept term.

3. Results

3.1. Whale Shark Surface Sightings and Identification

A total of 111 whale sharks were sighted in the Gulf of Tadjoura during the five-year study period, considering both new sightings and re-sightings.

Across the 111 sightings, 83 different specimens were detected: 5 in January 2017 (6.02%), 6 in January 2020 (7.23%), 27 in January 2022 (32.53%), 10 in November 2022 (12.05%), 33 in January 2024 (39.76%), and 2 in January 2025 (2.41%). No photo-identified individuals were re-sighted between 2017, 2020, and January 2022. In November 2022, 11 individuals (39.29%) were re-sighted, including 1 originally observed in January 2020 and 10 first sighted in January 2022. In 2024, 15 whale sharks (53.57%) were re-sighted, 2 of which were first recorded in 2020 and 13 in 2022 (11 from January 2022 and 2 from November 2022). In 2025, two specimens (7.14%) were re-sighted, one of which was first recorded in November 2022 and 1 in January 2024 (Figure 3).

Thus, each year contributed differently to the overall number of surface sightings; most of them occurred in January 2024 (43.24%), followed by January 2022 (24.32%), November 2022 (18.92%), January 2020 (5.41%), January 2017 (4.50%), and January 2025 (3.60%).

Only 1 specimen out of the 83 identified individuals was a female (1.20%) sighted in January 2025. The rest of the whale sharks (n = 82) whose sex was determined were males (98.80%).

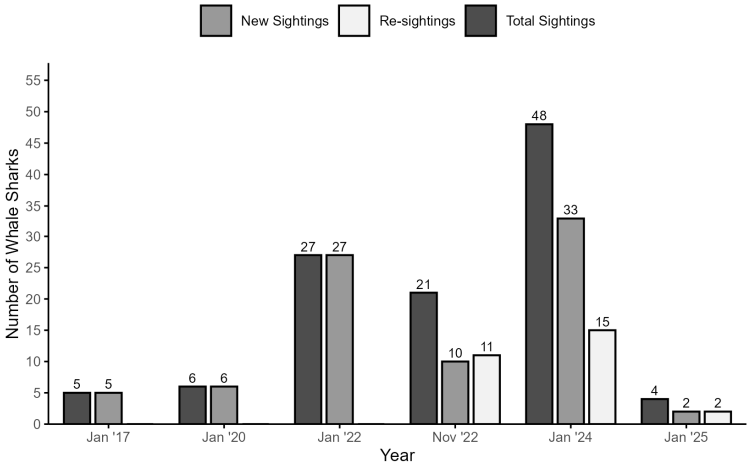

Figure 3. Number of total whale sharks sighted at surface, including new sightings and re-sightings, during the five-year study period.

Of the 83 photo-identified individuals, 39 specimens were measured for TL. In January 2022, 10 sharks averaged 6.14 ± 0.1 m; in November 2022, 9 sharks averaged 6.05 ± 0.1 m; in January 2024, 18 sharks averaged 6.4 ± 0.1 m; and in January 2025, 2 sharks averaged 6.46 ± 0.1 m. The overall mean TL across all measured sharks was 6.26 m ± 0.1, consistent with the size range of immature individuals [51].

Regarding the Wilcoxon Rank-Sum Test, the alternative hypothesis was rejected, indicating there were no significant differences (W = 101, p = 0.981) in the number of whale shark surface sightings influenced by environmental variables between January and November 2022. On the contrary, the Kruskal–Wallis test revealed a significant effect (K = 12.34, p = 0.015) of year on whale shark surface sightings, implying that the number of whale sharks sighted at the surface varied significantly among observation years.

3.2. Environmental Drivers of Whale Shark Surface Sightings

3.2.1. GAM Analysis

The initial GAM analysis included all seven predictors following the multicollinearity assessment (Table 1). Model selection, based on the highest percentage of variance explained, lowest AIC, and highest model weight, retained only three predictors of the original seven: SSC (chl-a), SST (temp), and wind strength (wind) (Table 2). The final model explained about 29.3% of the variability in the data (R^2 adj = 0.292596) and achieved the best overall performance (AIC = 254.4068). The relatively low variability explained by the GAM analysis may be due to the exclusion of some variables that were not considered in the present study.

Among the three predictors retained by the final model, the most significant factor was SST (temp), which accounted for more than half of the variance explained (19.5748%). SSC (chl-a) followed with the second-highest contribution to the explained variance, accounting for 9.2279%. Finally, wind strength (wind) explained a relatively small portion of the variability in the data (0.4973%); however, it was found to be statistically significant and thus retained in the final model (Table 3).

Table 2. Initial GAM analysis with model selection based on variance explained and AIC. "Model Covariates" lists the environmental variables included in each candidate model. Here, "temp" refers to SST, "wind" refers to wind strength, "chl-a" refers to SSC, "mei" refers to ENSO measurement unit (MEI), "sea" refers to sea condition, "okta" refers to brightness intensity, and "rain" refers to rainfall level; "K" denotes the number of estimated parameters including the intercept; "AIC" refers to the Akaike Information Criterion value for each model; "ΔAIC" represents the difference in AIC between a given model and the best-performing mode; "w_i" indicates the Akaike weight, representing the relative likelihood of each model given the data and the candidate set; and "R^2 adjusted (%)" reflects the percentage of variance explained by each model, adjusted for the number of parameters.

Model Covariates	K	AIC	ΔAIC	w_i	R^2 Adjusted (%)
chl-a + temp + wind	4	**254.4068**	0.0000	0.2963	**29.2596**
chl-a + mei + temp + wind	5	256.0312	1.6245	0.1315	28.2069
chl-a + okta + temp + wind	5	256.2332	1.8264	0.1189	28.5666
chl-a + rain + temp + wind	5	256.3316	1.9248	0.1131	28.2018
chl-a + temp	3	256.9647	2.5580	0.0825	28.5375
chl-a + mei + rain + temp + wind	6	257.1876	2.7809	0.0738	27.1402
chl-a + mei + okta + temp + wind	6	257.8474	3.4406	0.0530	27.5019
chl-a + sea conditions + temp + wind	6	258.1217	3.7149	0.0462	27.1400
chl-a + okta + rain + temp + wind	6	258.1861	3.7793	0.0448	27.4575
chl-a + rain + temp	4	258.4184	4.0116	0.0399	27.4672

Table 3. Contribution of each predictor to the variance explained in the final GAM model, including *p*-values and statistical significance. "Covariate" refers to the explanatory variables included in the model. Here, "temp" refers to SST, "chl-a" refers to SSC, and "wind" refers to wind strength; "Variance explained (%)" indicates the proportion of total variance explained by each covariate within the final GAM analysis; and "Pr(>|z|)" represents the associated *p*-value from a two-sided hypothesis test, where the null hypothesis corresponds to no significant effect.

Covariate	Variance Explained (%)	Pr(>|z|)
temp	19.5748	0.0000 ***
chl-a	9.2279	0.0000 ***
wind	0.4973	0.0479 **
Total	29.3000	/

(**) significance at 5%. (***) significance at 1%.

The outputs of the final GAM analysis highlighted how the main environmental predictors influenced the number of whale shark surface sightings (Table 4). The final model, which included SST (temp), SSC (chl-a), and wind strength (wind), explained the greatest variability in the data and had the lowest AIC (Table 2), indicating an optimal balance between goodness of fit and model parsimony.

Table 4. Outputs of the final GAM analysis, containing the covariates SST (temp), SSC (chl-a), and wind strength (wind). "Covariate" refers to the explanatory variables included in the model. Here, "temp" refers to SST, "chl-a" refers to SSC, and "wind" refers to wind strength; "Estimate" represents the estimated regression coefficients; "SE" represents Standard Error; "*z*-value" represents the test statistic obtained for each predictor (the ratio between "Estimate" and "SE"); and "Pr(>|z|)" represents the associated *p*-value from a two-sided hypothesis test, where the null hypothesis corresponds to no significant effect.

Covariate	Estimate	SE	*z*-Value	Pr(>|z|)
(Intercept)	−1.8773	0.3943	−4.7607	0.0000 ***
temp (1)	0.9151	0.1966	4.6537	0.0000 ***
wind (1)	0.6101	0.3084	1.9781	0.0479 **
chl-a (1)	1.8716	0.2786	6.7180	0.0000 ***

(**) significance at 5%. (***) significance at 1%.

Table 4 summarises the final model outputs, where two of the covariates retained in the final model, temp (SST) and chl-a (SSC), were significant at 1%, emphasizing the efficiency of this statistical approach in capturing the relationships between the number of whale shark surface sightings and environmental drivers. The model was fitted using a Poisson distribution with a log link function, which is appropriate for count data, such as whale shark surface sightings. The log link ensured that predicted counts remained positive and allowed covariate effects to be interpreted as multiplicative changes on the original count scale. Therefore, the estimated coefficients ("Estimates") represent changes in the log of the expected number of sightings relative to the reference level for each categorical covariate ($\leq$0.5 mg/m^3 for chl-a, $\leq$26 °C for temp, and <7 knots for wind). Exponentiating these "Estimates" allows interpretation on the original scale, indicating how many times higher (or lower) the expected number of whale shark surface sightings is for each predictor level compared to the baseline. Specifically, the expected number of surface sightings was approximately 6.5 times higher when SSC was >0.5 mg/m^3, 2.5 times higher when SST was >26 °C, and 1.8 times higher when wind strength was $\geq$7 knots, relative to their respective reference categories. The positive *z*-values suggested a significant effect of each covariate retained in the model on whale shark surface sightings. As reported in Table 4, all *t*-values exceeded the conventional threshold of $\pm$1.96 for a significance level of 5%. SSC (chl-a, *z*-value = 6.7180) and SST (temp, *z*-value = 4.6537) displayed the largest *t*-values, implying that both predictors consistently and robustly influenced whale shark relative abundance, whereas wind strength (wind, *z*-value = 1.9781) exhibited a lower *t*-value, implying a weaker and more complex effect on surface sightings. Finally, as shown in Table 4, both SSC and SST were highly significant ($p < 0.001$), providing strong evidence that when SSC was >0.5 mg/m^3 and SST > 26 °C, the number of whale shark surface sightings in the Gulf of Tadjoura considerably increased across all the years. Wind strength also had a statistically robust effect ($p < 0.05$), even though it was much weaker than the other variables included in the model. However, the effect of wind strength on surface sightings is not negligible and is still associated with a higher presence of specimens at the surface in the Gulf of Tadjoura (Figure 4).

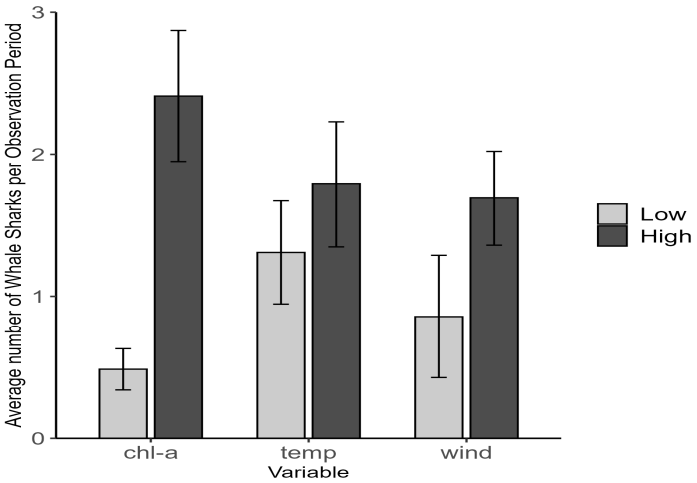

Figure 4. Average number of whale sharks sighted at the surface per observation period under low and high SSC (chl-a), SST (temp), and wind strength (wind) conditions. "High" conditions correspond to chl-a > 0.5 mg/m^3, temp > 26 °C, and wind $\geq$ 7 knots. "Low" conditions denote chl-a $\leq$ 0.5 mg/m^3, temp $\leq$ 26 °C, and wind < 7. Error bars represent standard error.

3.2.2. Hurdle Model

The first step of the Hurdle model evaluated the most appropriate distribution for the second component of the model based on the data available. In this context, two alternative

specifications were compared, namely Hurdle Poisson and Hurdle Negative Binomial, each containing seven predictors in both components of the model. Best distribution selection considered AIC and BIC. According to Table 5, the Hurdle Poisson specification (AIC = 235.4666; BIC = 276.4466) provided a better balance between fit and complexity; therefore, it was selected for the second step of the analysis.

Table 5. Comparison of alternative distributional specifications for the count component of the Hurdle model based on AIC and BIC criteria. "Distribution" denotes the two different Hurdle specifications fitted with different distributional assumptions; "AIC" refers to Akaike's information criterion; and "BIC" denotes the Bayesian information criterion.

Distribution	AIC	BIC
Hurdle Poisson	235.4666	276.4466
Hurdle Negative Binomial	236.4240	279.6807

Following this choice, sighting data were modelled using a two-part Hurdle specification: a Bernoulli–logit model for the probability of at least one sighting and, conditional on presence, a zero-truncated Poisson model with log link for positive counts. Variable selection was then performed separately for the two components (AIC-based stepwise): the zero-component retained SSC and SST, whereas the count component retained SSC, SST, and wind strength (Tables 6–9).

Table 6. Stepwise variable selection for the zero-component Hurdle model (Binomial GLM). "Model Covariates" lists the predictor variables included in each candidate model. Here, "temp" refers to SST, "wind" refers to wind strength, "chl-a" refers to SSC, "mei" refers to ENSO measurement unit (MEI), "sea" refers to sea condition, "okta" refers to brightness intensity, and "rain" refers to rainfall level; "K" denotes the number of estimated parameters including the intercept; "AIC" refers to the Akaike Information Criterion value for each model.

Model Covariates	K	AIC
temp + wind + mei + chl-a + sea conditions + okta + rain	8	103.5916
chl-a + mei + rain + sea conditions + temp + wind	7	101.6025
chl-a + mei + rain + temp + wind	6	100.7984
chl-a + mei + rain + temp	5	99.2433
chl-a + mei + temp	4	98.5326
chl-a + temp	3	**96.8446**

Table 7. Stepwise variable selection for the count component Hurdle model (Poisson GLM). "Model Covariates" lists the predictor variables included in each candidate model. Here, "temp" refers to SST, "wind" refers to wind strength, "chl-a" refers to SSC, "mei" refers to ENSO measurement unit (MEI), "sea" refers to sea condition, "okta" refers to brightness intensity, and "rain" refers to rainfall level; "K" denotes the number of estimated parameters, including the intercept; "AIC" refers to the Akaike Information Criterion value for each model.

Model Covariates	K	AIC
temp + wind + mei + chl-a + sea conditions + okta + rain	8	262.5767
chl-a + mei + okta + rain + temp + wind	7	259.1028
chl-a + mei + rain + temp + wind	6	257.1876
chl-a + mei + temp + wind	5	256.0312
chl-a + temp + wind	4	**254.4068**

Table 8. GLM summary statistics for zero-component (Binomial, logit link) of the final Hurdle Model. "Covariate" refers to the explanatory variables included in the model; here, "temp" refers to SST and "chl-a" refers to SSC; "Estimate" stands for the estimated regression coefficients; "SE" represents Standard Error; "*z*-value" represents the test statistic obtained for each predictor (the ratio between "Estimate" and "SE"); and "Pr(>|z|)" represents the associated *p*-value from a two-sided hypothesis test, where the null hypothesis corresponds to no significant effect.

Covariate	Estimate	SE	*z*-Value	*p*-Value
(Intercept)	−1.4583	0.5848	−2.4937	0.0126 *
chl-a (1)	1.5905	0.5908	2.6919	0.0071 **
temp (1)	0.8837	0.5867	1.5064	0.1320

(*) significance at 10%. (**) significance at 5%.

Table 9. GLM summary statistics for count component (Zero-truncated Poisson, log link) of the final Hurdle Model. Here, "Covariate" refers to the explanatory variables included in the model. Here, "temp" refers to SST, "chl-a" refers to SSC, and "wind" refers to wind strength; "Estimate" represents the estimated regression coefficients; "SE" stands for Standard Error; "*z*-value" stands for the test statistic obtained for each predictor (the ratio between "Estimate" and "SE"); and "Pr(>|z|)" represents the associated *p*-value from a two-sided hypothesis test, where the null hypothesis corresponds to no significant effect.

Covariate	Estimate	SE	z-value	*p*-value
(Intercept)	−0.9776	0.5435	−1.7987	0.0721
temp (1)	0.5787	0.2132	2.7139	0.0066 **
wind (1)	0.7567	0.3954	1.9141	0.0556
chl-a (1)	1.4180	0.4011	3.5355	0.0004 ***

(**) significance at 5%. (***) significance at 1%.

This approach allowed the independent modelling of the ecological drivers influencing whale shark surface occurrence (zero component) and relative abundance (count component) in the Gulf of Tadjoura.

A stepwise variable selection based on AIC for the zero-component retained only two of the original seven predictors: SSC (chl-a) and SST (temp) (Table 6). According to Table 6, the binomial GLM containing these two variables yielded the lowest AIC (AIC = 96.8446), indicating the best balance between goodness of fit and model complexity.

Regarding the count component, stepwise AIC selection retained three predictors: SSC (chl-a), SST (temp), and wind strength (wind) (Table 7). As shown in Table 7, the Poisson GLM, including these three variables, exhibited the lowest AIC (AIC = 254.4068).

The final Hurdle model provided valuable insights regarding the environmental drivers of whale shark surface occurrence and relative abundance in the Gulf of Tadjoura. The zero component, which modelled the surface presence/absence patterns, retained only two drivers, SSC (chl-a) and SST (temp), suggesting their key role in controlling occurrence patterns (Table 8).

Table 8 displays the GLM model outputs for the final Hurdle model (zero-component), which was fitted using a Binomial distribution with a logit link function, suitable for modelling binary outcomes such as whale shark surface absence or presence. The logit link function converts the probability of surface presence/absence into a linear function of the predictors on the log-odds scale. In addition, it restricts the predicted probabilities between 0 and 1, while ensuring the interpretation of the covariates' effects as multiplicative changes in odds on the original scale. Therefore, the estimated coefficients ("Estimates") denoted changes in the log-odds of whale shark surface presence relative to the reference level for each categorical covariate ($\leq$0.5 mg/m^3 for SSC, and $\leq$26 °C for SST). Exponentiating these "Estimates" yields an interpretation on the odds scale, indicating how many times higher (or

lower) the odds of whale shark surface occurrence are for each predictor level compared to the baseline. Notably, the odds of whale shark presence were approximately 4.9 times higher when SSC was >0.5 mg/m^3 and 2.4 times higher when SST was >26 °C, relative to their respective reference categories. Regarding *z*-values, SSC (chl-a, *z*-value = 2.6919) exhibited a strong positive effect, whereas the variable SST (temp, *z*-value = 1.5064) displayed a slightly weaker effect. The corresponding *p*-values support this interpretation: SSC ($p = 0.0071$) was statistically significant at 5%, providing evidence of its key role in positively influencing whale shark surface occurrence in the Gulf of Tadjoura. Conversely, SST was not significant ($p = 0.1320$), suggesting a weaker influence on surface occurrence patterns.

On the contrary, the count component, which described the number of surface sightings when at least one specimen was present, retained SSC (chl-a), SST (temp), and wind strength (wind) underlying their importance in shaping whale shark relative abundance (Table 9).

Table 9 presents the GLM model outputs for the count component of the final Hurdle model, which was fitted using a Poisson distribution with a log link function, appropriate for modelling count data such as whale shark surface sightings. The log link ensures that predicted counts remain positive and allows covariate effects to be interpreted as multiplicative changes in the expected count. Thus, the estimated coefficients ("Estimates") represent changes in the log of the expected number of sightings relative to the reference level for each categorical covariate ($\leq$0.5 mg/m^3 for SSC, $\leq$26 °C for SST, and <7 knots for wind strength). Exponentiating these "Estimates" provides an interpretation of the original count scale, indicating how many times higher (or lower) the expected number of sightings is compared to the baseline. Notably, the expected number of sightings was approximately 4.1 times higher when SSC was >0.5 mg/m^3, 1.8 times higher when SST was >26 °C, and 2.1 times higher when wind strength was $\geq$7 knots. Based on *z*-values, SSC (chl-a, *z*-value = 3.5355) and SST (temp, *z*-value = 2.7139) exceeded the conventional threshold of $\pm$1.96 for a significance level of 5%, suggesting a strong influence on the number of surface sightings. The covariate wind strength (wind, *z*-value = 1.9141) exhibited a comparatively weaker effect on the number of surface sightings; however, it remained positively associated with whale shark relative abundance. These findings were supported by the *p*-values: both SSC ($p = 0.0004$) and SST ($p = 0.0066$) were significant at 1% and 5%, respectively, highlighting their influence on surface sightings when at least one individual was sighted. The predictor wind strength ($p = 0.0556$) was not significant; however, its positive *z*-value and proximity to the significance threshold indicate a weaker association with the number of whale shark surface sightings in the Gulf of Tadjoura.

4. Discussion

This study is the first to thoroughly examine the environmental factors influencing immature whale shark surface sightings in the Gulf of Tadjoura. The 83 specimens identified provide further evidence that Djibouti represents a key seasonal aggregation site for this species, as previously highlighted by Micarelli et al. [29], Boldrocchi et al. [30], Rowat et al. [28], and Reinero et al. [31].

The re-sighting of 28 whale sharks (25.2% of identified sharks) throughout the study period suggests that certain individuals remain in the region for extended periods, as previously noted by Rowat et al. [28], Boldrocchi et al. [30] and Reinero et al. [31]. Furthermore, by deploying eight pop-up satellite tags on whale sharks in the Gulf of Tadjoura, Andrzejaczek et al. [35] showed that individuals remained near the aggregation site for up to one month and left the area only around February, likely in response to declining food availability. Similarly, Rowat et al. [52] showed a limited whale shark dispersion during the off-season from Djibouti to the Red Sea and the northern Indian Ocean.

The average TL (6.26 m ± 0.1) of whale sharks in the Gulf of Tadjoura and the only female specimen identified over the five-year study period confirm a size- and sex-based aggregation in favor of immature males [26,28,30,31]. Size- and sex-based segregation is well-documented for shark species due to different dietary requirements [53], reduced intra-specific competition [54], reproductive strategies [55] and thermal preferences [56]. Females are occasionally sighted in Djibouti [28,30], and male bias remains poorly understood. However, Meekan et al. [57] stated that enhanced feeding opportunities for male whale sharks in coastal waters, along with associated benefits of faster growth and increased reproductive success, might outweigh the higher predation risks, while females prefer to adopt a more conservative strategy prioritizing slower but steady growth while minimizing risks. Previous studies suggested no differences in terms of whale shark dietary preferences [58], habitat use [59], and behavior [60] at coastal aggregation sites. Unravelling the dynamics that drive sex- and size-segregation for this species is complicated due to the elusive and wide-ranging behavior of whale sharks that makes direct observations and long-term monitoring particularly challenging. In this context, studies integrating satellite telemetry to monitor whale shark movements and stable isotope analysis to explore trophic ecology could provide novel insights into this topic.

The strong positive correlation between SSC and immature whale shark surface occurrence and relative abundance across the study period may indicate that both presence and sightings should be correlated with periods of high food availability in coastal areas [28,30,61–64]. For instance, in the Gulf of Tadjoura, Boldrocchi et al. [30] showed a positive correlation between monthly SSC obtained from satellite data and collected zooplankton biomass. Although direct measurements of zooplankton biomass were not directly measured in this study, Copernicus satellite-derived SSC data indicated higher mean concentrations values in January 2022 (0.54 mg/m^3), November 2022 (2.18 mg/m^3), and 2024 (0.61 mg/m^3) with respect to 2017 (0.25 mg/m^3), 2020 (0.47 mg/m^3), and 2025 (0.43 mg/m^3). Given that immature whale shark surface occurrence and relative abundance were significantly higher when SSC exceeded 0.5 mg/m^3, this threshold may account for the increased presence and sightings observed in 2022 and 2024 compared to 2017, 2020, and 2025. Additional evidence supporting a positive association between SSC and whale shark relative abundance has been documented in several aggregation sites, including the Seychelles [19], Ningaloo Reef [36], Gulf of Mexico [65], Indonesia [40], and Djibouti [30]. Although statistical modelling could estimate the SSC threshold below which the presence and relative abundance of immature whale sharks are unlikely to occur, a more detailed investigation on the correlation between zooplankton biomass and daily immature whale shark surface occurrence and sightings in Djiboutian waters is required to obtain necessary insights into potential interaction effects. Furthermore, given the opportunistic foraging behavior of whale sharks and their tendency to aggregate in areas of high zooplankton biomass [30,66,67], detection of such productive areas is also crucial.

Similar to SSC, SST exhibited a significant influence on whale shark distribution, with relative abundance and occurrence increasing when SST exceeded the 26 °C threshold across the study period. Indeed, the highest number of whale shark surface sightings was in 2024 (43.24%) when the mean SST (27.9 °C) was the highest recorded. However, in January 2022 and November 2022, although sightings were also high (24.32% and 18.92%, respectively), the mean SST (25.9 °C) did not exceed the 26 °C threshold. Conversely, while sightings were low in 2017, 2020, and 2025 (4.50%, 5.41% and 3.60%, respectively), mean SST exceeded the 26 °C threshold in all three years (mean SST in 2017 = 26.1 °C; in 2020 = 26.2°; and in 2025 = 26.5 °C). Together, these patterns indicate that although SST contributes to shaping the relative abundance of whale sharks in the area, it should be interpreted in conjunction with SSC, which also exerts a significant influence. For instance,

although the highest mean SSC was in November 2022 (2.18 mg/m^3), mean SST during this period was lower (25.9 °C) by 2 degrees than in January 2024 (27.9 °C), when the highest number of sightings was recorded. In the other years (2017, 2020, January 2022, and 2025), mean SST and SSC were always lower than those recorded in 2024. These observations suggest that a complex interaction between these two main environmental parameters exists and influences patterns of whale shark surface sightings in the Gulf of Tadjoura.

Overall, results indicate that the optimal SST for immature individuals seasonally aggregating in this area likely ranges between 26 °C and 29 °C, which falls within the reported preferred thermal range for whale sharks of 18–32 °C [36,40,42,43,68,69]. Despite their broad thermal tolerance, whale sharks habitually spend time in surface waters to maintain exposure to an optimal thermal range [17,39,70]. However, deep dives beyond this preferred thermal range have been frequently observed, likely resulting from whale shark vertical movements associated with foraging on mesopelagic prey when food availability declines at the surface [71] or from thermoregulatory behavior linked to the whale shark's ectothermic physiology [72].

Besides affecting whale shark physiology and metabolism [17,70], SST could enhance the availability at the surface of certain prey items, thereby increasing whale shark surface sightings. Notably, warmer SSTs have been associated with increased productivity in the marine environment, favoring localized concentrations of zooplankton blooms and fish spawning events [22,61–63,73]. In the Gulf of Tadjoura, higher immature whale shark surface sightings linked to SST exceeding the 26 °C threshold could reflect the influence of monsoon-driven upwelling on primary productivity and prey availability in Djibouti [31,32,74–78], although this aspect needs to be further investigated. Similarly, in Ningaloo Reef, D'Antonio et al. [79] stated that the thermal front driven by the convergence of the warm Leeuwin Current waters and the cooler Ningaloo Current [80,81] induces localized upwelling, which enhances productivity in warm surface waters close to the reef [44,82,83], attracting whale sharks.

However, mechanisms by which SST affects prey availability and, consequently, whale shark relative abundance vary across aggregation sites or specific prey items. For instance, in the São Pedro and São Paulo Archipelago (equatorial Atlantic), whale shark surface sightings increased under elevated SST, reduced current speeds, and low SSC values, conditions that favor fish and invertebrate spawning [84]. Similarly, at the Al Shaheen oil field in the Arabian Gulf, whale shark aggregation occurs when SST ranges between 27–33 °C due to the highest densities of mackerel tuna eggs on which this species feeds [66]. At Isla Contoy in the Mexican Caribbean, spawning of little tunny linked to higher SSTs was also associated with increased whale shark surface sightings [63]. Thus, additional studies are required to assess whether certain SST thresholds could affect the distribution of surface prey and, consequently, the frequency of immature whale shark surface sightings in the Gulf of Tadjoura.

Although whale shark sightings in the Gulf of Tadjoura have always occurred within 50 m offshore, bathymetric gradients represent important habitats for whale sharks [43]. This species is well-known to occur in areas with dynamic oceanography, such as regions of oceanic mixing within upwelling habitats [43]. Even if bathymetric gradients were not considered during whale shark surface surveys, as sampling always took place within 50 m offshore, Omar et al. [85] suggested that monsoon winds and their seasonal reversal are the primary drivers of surface circulation in the west of the Gulf of Aden. However, monsoons in the Gulf of Tadjoura are governed essentially by topography and influence in turn SST and SSC variations at the surface [85]. The basin of the Gulf of Tadjoura is bowl-shaped, elongated along the east–west axis, and shallower in the west. This strengthens the wind stress on the western side, where a significant volume of surface water is moved [85].

Considering such water displacements and given the strict positive correlation between SST and dissolved oxygen along depth gradients in the Gulf of Tadjoura [85], further investigations on bathymetric and coastal distance parameters influencing whale shark surface sightings, as well as the effects of dissolved oxygen and current strength and direction, are required.

Unlike SSC and SST, which have emerged as consistent predictors of immature whale shark surface sightings in the Gulf of Tadjoura, wind strength appeared to have a weaker and more complex effect across the study period. Aside from the significant increase in immature whale shark relative abundance when wind strength was equal to or greater than 7 knots, its influence was limited. Thus, the positive effect observed may reflect localized, short-term wind conditions that promote surface mixing and nutrient enrichment without exceeding disruptive thresholds. For instance, the influence of wind on whale shark coastal aggregations appeared to be different depending on the locations, sometimes having a positive [37] or negative [19] relationship with whale shark surface sightings.

5. Conclusions

Investigating the environmental drivers of whale shark surface sightings can be challenging, especially because relative abundance is used as a proxy for absolute abundance, which may introduce bias when evaluating temporal and spatial patterns in surface occurrence. Findings suggest that SSC and SST could predict immature whale shark surface occurrence and sightings in the Gulf of Tadjoura across the study period, although further investigations into the effects of zooplankton biomass and other prey items driven by specific environmental variable thresholds are required to better understand their role in shaping the relative abundance and presence of this species. Since prey availability is the main driver of whale shark seasonal aggregations, environmental changes could exert a significant influence on prey distribution and abundance and, consequently, on the species' occurrence and sightings at the surface. Therefore, further and deeper analyses should be conducted to examine other environmental variables and/or broader oceanographic and atmospheric processes, such as dissolved oxygen, bathymetry, coastal distance, monsoons, and current strength and direction, that might influence whale shark surface sightings, and which were not taken into consideration in the present study. Given the crucial role of environmental factors in modelling whale shark relative abundance, a key tool for inferring habitat use and movement patterns of this species and supporting the rapid development of whale shark ecotourism, improving our understanding of these influences could help to clarify temporal and seasonal trends in whale shark presence and develop conservation strategies to protect this endangered species within the Gulf of Tadjoura.

Author Contributions: Conceptualization, F.R.R. and P.M.; methodology, F.R.R., P.M. and A.M.; software, A.P., G.V., F.R.R. and P.M.; validation, F.R.R., P.M., A.M.; formal analysis, A.P. and G.V.; investigation, F.R.R., P.M., A.M. and G.V.; resources, P.M., F.R.R., A.M.; data curation, F.R.R., P.M., A.M., G.V. and A.P.; writing—original draft preparation, F.R.R.; writing—review and editing, F.R.R., P.M., A.M., G.V., A.P. and M.M.; supervision, F.R.R., P.M. and A.M. All authors have read and agreed to the published version of the manuscript.

Funding: This research received no external funding.

Institutional Review Board Statement: Ethical review and approval were waived for this study by Sharks Studies Centre-Scientific Institute due to it did not intervene in the observed animals.

Informed Consent Statement: Not applicable.

Data Availability Statement: Data will be available after publication on ResearchGate after request to the authors.

Acknowledgments: We are grateful to the Sharks Studies Centre-Scientific Institute team members that carried out the expeditions for their indirect financial support of this research, and thanks are also due to the "Elegante" boat's team for the logistical and field assistance with data collection, and to Francesca Ellero for her thorough English revision.

Conflicts of Interest: The authors declare no conflicts of interest.

References

1. Heupel, M.R.; Knip, D.M.; Simpfendorfer, C.A.; Dulvy, N.K. Sizing up the Ecological Role of Sharks as Predators. *Mar. Ecol. Prog. Ser.* **2014**, *495*, 291–298. [CrossRef]
2. Monteforte, K.I.P.; Butcher, P.A.; Morris, S.G.; Kelaher, B.P. The Relative Abundance and Occurrence of Sharks off Ocean Beaches of New South Wales, Australia. *Biology* **2022**, *11*, 1456. [CrossRef] [PubMed]
3. Myers, R.A.; Baum, J.K.; Shepherd, T.D.; Powers, S.P.; Peterson, C.H. Cascading Effects of the Loss of Apex Predatory Sharks from a Coastal Ocean. *Science* **2007**, *315*, 1846–1850. [CrossRef]
4. Baum, J.K.; Worm, B. Cascading top-down effects of changing oceanic predator abundances. *J. Anim. Ecol.* **2009**, *78*, 699–714. [CrossRef]
5. Polovina, J.J.; Abecassis, M.; Howell, E.A.; Woodworth, P. Increases in the Relative Abundance of Mid-Trophic Level Fishes Concurrent with Declines in Apex Predators in the Subtropical North Pacific, 1996–2006. *Fish. Bull.* **2009**, *107*, 523–531.
6. Ferretti, F.; Worm, B.; Britten, G.L.; Heithaus, M.R.; Lotze, H.K. Patterns and ecosystem consequences of shark declines in the ocean. *Ecol. Lett.* **2010**, *13*, 1055–1071. [CrossRef]
7. Stevens, J.; Bonfil, R.; Dulvy, N.K.; Walker, P. The effects of fishing on sharks, rays, and chimaeras (chondrichthyans), and the implications for marine ecosystems. *ICES J. Mar. Sci.* **2000**, *57*, 476–494. [CrossRef]
8. Desbiens, A.A.; Roff, G.; Robbins, W.D.; Taylor, B.M.; Castro-Sanguino, C.; Dempsey, A.; Mumby, P.J. Revisiting the Paradigm of Shark-Driven Trophic Cascades in Coral Reef Ecosystems. *Ecology* **2021**, *102*, e03303. [CrossRef]
9. Dulvy, N.K.; Pacoureau, N.; Rigby, C.L.; Pollom, R.A.; Jabado, R.W.; Ebert, D.A.; Finucci, B.; Pollock, C.M.; Cheok, J.; Derrick, D.H.; et al. Overfishing Drives over One-Third of All Sharks and Rays toward a Global Extinction Crisis. *Curr. Biol.* **2021**, *31*, 4773–4787. [CrossRef] [PubMed]
10. Simpfendorfer, C.A.; Heithaus, M.R.; Heupel, M.R.; MacNeil, M.A.; Meekan, M.; Harvey, E.; Sherman, C.S.; Currey-Randall, L.M.; Goetze, J.S.; Kiszka, J.J.; et al. Widespread diversity deficits of coral reef sharks and rays. *Science* **2023**, *380*, 1155–1160. [CrossRef]
11. Dunson, W.A.; Travis, J. The Role of Abiotic Factors in Community Organization. *Am. Nat.* **1991**, *138*, 1067–1091. [CrossRef]
12. Schlaff, A.M.; Heupel, M.R.; Simpfendorfer, C.A. Influence of Environmental Factors on Shark and Ray Movement, Behaviour and Habitat Use: A Review. *Rev. Fish. Biol. Fish.* **2014**, *24*, 1089–1103. [CrossRef]
13. Reyes-Mendoza, O.; Cárdenas-Palomo, N.; Herrera-Silveira, J.; Mimila-Herrera, E.; Trujillo-Córdova, J.; Chiappa-Carrara, X.; Arceo-Carranza, D. Quantity and Quality of Prey Available for the Whale Shark (*Rhincodon typus*, Smith 1828) at the Mexican Caribbean Aggregation Site. *Reg. Stud. Mar. Sci.* **2021**, *43*, 101696. [CrossRef]
14. Callaghan, C.T.; Santini, L.; Spake, R.; Bowler, D.E. Population abundance estimates in conservation and biodiversity research. *Trends Ecol. Evol.* **2024**, *39*, 515–523. [CrossRef]
15. Shea, B.D.; Benson, C.W.; De Silva, C.; Donovan, D.; Romeiro, J.; Bond, M.E.; Creel, S.; Gallagher, A.J. Effects of Exposure to Large Sharks on the Abundance and Behavior of Mobile Prey Fishes along a Temperate Coastal Gradient. *PLoS ONE* **2020**, *15*, e0230308. [CrossRef]
16. Stevens, J.D.; Bradford, R.W.; West, G.J. Satellite tagging of blue sharks (*Prionace glauca*) and other pelagic sharks off eastern Australia: Depth behaviour, temperature experience and movements. *Mar. Biol.* **2010**, *157*, 575–591. [CrossRef]
17. Tyminski, J.P.; de la Parra-Venegas, R.; González Cano, J.; Hueter, R.E. Vertical Movements and Patterns in Diving Behavior of Whale Sharks as Revealed by Pop-Up Satellite Tags in the Eastern Gulf of Mexico. *PLoS ONE* **2015**, *10*, e0142156. [CrossRef]
18. Coffey, D.M.; Royer, M.A.; Meyer, C.G.; Holland, K.N. Diel Patterns in Swimming Behavior of a Vertically Migrating Deepwater Shark, the Bluntnose Sixgill (*Hexanchus griseus*). *PLoS ONE* **2020**, *15*, e0228253. [CrossRef]
19. Rowat, D.; Gore, M.; Meekan, M.G.; Lawler, I.R.; Bradshaw, C.J.A. Aerial survey as a tool to estimate whale shark abundance trends. *J. Exp. Mar. Bio. Ecol.* **2009**, *368*, 1–8. [CrossRef]
20. Witt, M.J.; Hardy, T.; Johnson, L.; McClellan, C.M.; Pikesley, S.K.; Ranger, S.; Richardson, P.B.; Solandt, J.-L.; Speedie, C.; Williams, R.; et al. Basking Sharks in the Northeast Atlantic: Spatio-Temporal Trends from Sightings in UK Waters. *Mar. Ecol. Prog. Ser.* **2012**, *459*, 121–134. [CrossRef]
21. Robbins, W.D.; Peddemors, V.M.; Kennelly, S.J.; Ives, M.C. Experimental evaluation of shark detection rates by aerial observers. *PLoS ONE* **2014**, *9*, e83456. [CrossRef]

22. Maruanaya, Y.; Retraubun, A.S.W.; Tuhumury, S.F.; Abrahamsz, J. Characteristics and the Appearance of New Whale Sharks (*Rhincodon typus*) as a Unique Phenomenon in the Kwatisore Waters within the Cenderawasih Bay National Park Area, Papua. *Tomini J. Aquat. Sci.* **2021**, *2*, 24–40. [CrossRef]
23. Nykänen, M.; Jessopp, M.; Doyle, T.K.; Harman, L.A.; Cañadas, A.; Breen, P.; Hunt, W.; Mackey, M.; Cadhla, O.Ó.; Reid, D.; et al. Using Tagging Data and Aerial Surveys to Incorporate Availability Bias in the Abundance Estimation of Blue Sharks (*Prionace glauca*). *PLoS ONE* **2018**, *13*, e0203122. [CrossRef]
24. Westgate, A.J.; Koopman, H.N.; Siders, Z.A.; Wong, S.N.P.; Ronconi, R.A. Population density and abundance of basking sharks *Cetorhinus maximus* in the lower Bay of Fundy, Canada. *Endanger. Species Res.* **2014**, *23*, 177–185. [CrossRef]
25. Notarbartolo di Sciara, G.; Lauriano, G.; Pierantonio, N.; Cañadas, A.; Donovan, G.; Panigada, S. The Devil We Don't Know: Investigating Habitat and Abundance of Endangered Giant Devil Rays in the North-Western Mediterranean Sea. *PLoS ONE* **2015**, *10*, e0141189. [CrossRef]
26. Rowat, D.; Meekan, M.G.; Engelhardt, U.; Pardigon, B.; Vely, M. Aggregations of juvenile whale sharks (*Rhincodon typus*) in the Gulf of Tadjoura, Djibouti. *Environ. Biol. Fishes* **2007**, *80*, 465–472. [CrossRef]
27. Rezzolla, D.; Storai, T. "Whale Shark Expedition": Observations on *Rhincodon typus* from Arta Bay, Gulf of Tadjoura, Djibouti Republic, Southern Red Sea. *Cybium* **2010**, *34*, 195–206.
28. Rowat, D.; Brooks, K.; March, A.; McCarten, C.; Jouannet, D.; Riley, L.; Jeffreys, G.; Perri, M.; Vely, M.; Pardigon, B. Long-term membership of whale sharks (*Rhincodon typus*) in coastal aggregations in Seychelles and Djibouti. *Mar. Fresh. Res.* **2011**, *62*, 621–627. [CrossRef]
29. Micarelli, P.; Romano, C.; Buttino, I.; Reinero, F.; Serangeli, C.; Sperone, E. Phytoplanktonbloom and seasonal presence of whale shark (*Rhincodon typus*) along the coast of Djibouti-Gulf of Aden. *Int. J. Curr. Adv. Res.* **2017**, *6*, 3948–3949. [CrossRef]
30. Boldrocchi, G.; Omar Moussa, Y.; Azzola, A.; Bettinetti, R. The ecology of the whale shark in Djibouti. *Aquat. Ecol.* **2020**, *54*, 535–551. [CrossRef]
31. Reinero, F.R.; Marsella, A.; Pacifico, A.; Vicariotto, C.; Maule, L.; Mahrer, M.; Micarelli, P. Influence of Environmental Factors on the Surface Feeding Behaviour of Immature Male Whale Sharks in the Gulf of Tadjoura (Djibouti). *Conservation* **2024**, *4*, 792–811. [CrossRef]
32. Boldrocchi, G.; Omar Moussa, Y.; Rowat, D.; Bettinetti, R. First results on zooplankton community composition and contamination by some persistent organic pollutants in the Gulf of Tadjoura (Djibouti). *Sci. Total Environ.* **2018**, *627*, 812–821. [CrossRef]
33. Di Capua, I.; Micarelli, P.; Tempesti, J.; Reinero, F.R.; Buttino, I. Zooplankton size structure in the Gulf of Tadjoura (Djibouti) during whale shark sighting: A preliminary study. *Cah. Biol. Mar.* **2021**, *62*, 290–294. [CrossRef]
34. Boldrocchi, G.; Bettinetti, R. Whale shark foraging on baitfish off Djibouti. *Mar. Biodivers.* **2019**, *49*, 2013–2016. [CrossRef]
35. Andrzejaczek, S.; Vély, M.; Jouannet, D.; Rowat, D.; Fossette, S. Regional Movements of Satellite-Tagged Whale Sharks *Rhincodon typus* in the Gulf of Aden. *Ecol. Evol.* **2021**, *11*, 4920–4934. [CrossRef] [PubMed]
36. Sleeman, J.C.; Meekan, M.G.; Wilson, S.G.; Jenner, C.K.; Jenner, M.N.; Boggs, G.S.; Steinberg, C.C.; Bradshaw, C.J.A. Biophysical Correlates of Relative Abundances of Marine Megafauna at Ningaloo Reef, Western Australia. *Mar. Freshw. Res.* **2007**, *58*, 608–623. [CrossRef]
37. Sleeman, J.C.; Meekan, M.G.; Fitzpatrick, B.J.; Steinberg, C.R.; Ancel, R.; Bradshaw, C.J.A. Oceanographic and atmospheric phenomena influence the abundance of whale sharks at Ningaloo Reef, Western Australia. *J. Exp. Mar. Biol. Ecol.* **2010**, *382*, 77–81. [CrossRef]
38. Rohner, C.A.; Pierce, S.J.; Marshall, A.D.; Weeks, S.J.; Bennett, M.B.; Richardson, A.J. Trends in sightings and environmental influences on a coastal aggregation of manta rays and whale sharks. *Mar. Ecol. Prog. Ser.* **2013**, *482*, 153–168. [CrossRef]
39. Gibson, S. The Influence of Environmental and Anthropogenic Variables on Whale Shark *(Rhincodon typus)* Abundance in the South Ari Atoll. Ph.D. Thesis, University of Plymouth, Plymouth, UK, 2017.
40. Manuhutu, J.F.; Wiadnya, D.G.R.; Sambah, A.B.; Herawati, E.Y. The presence of whale sharks based on oceanographic variations in Cenderawasih Bay National Park, Papua, Indonesia. *Biodiversitas* **2021**, *22*, 4948–4955. [CrossRef]
41. Swai, E.; Alavaisha, E. Environmental factors influencing the sightings of whale shark (*Rhincodon typus*, Smith 1828): The case study in Kilindoni Bay, Mafia District, Tanzania. University of Dar es Salaam, Dar es Salaam, Tanzania. *Res. Sq.* **2024**. [CrossRef]
42. Sequeira, A.; Mellin, C.; Rowat, D.; Meekan, M.G.; Bradshaw, C.J.A. Ocean-scale prediction of whale shark distribution. *Divers. Distrib.* **2012**, *18*, 504–518. [CrossRef]
43. Milles, H.M.; Hoffmayer, E.R.; Arostegui, M.C.; de la Parra-Venegas, R.; Driggers, W.B., III; Franks, J.S.; Graham, R.T.; Hendon, J.M.; McKinney, J.A.; Olton, M.; et al. Characterizing seasonal whale shark habitat in the western North Atlantic. *Mar. Ecol. Progr. Ser.* **2025**, *766*, 91–106. [CrossRef]
44. Wilson, S.G.; Taylor, J.G.; Pearce, A.F. The seasonal aggregation of whale sharks at Ningaloo Reef, Western Australia: Currents, migrations and the El Niño/ Southern Oscillation. *Environ. Biol. Fishes* **2001**, *61*, 1–11. [CrossRef]
45. Elith, J.; Phillips, S.J.; Hastie, T.; Dudík, M.; Chee, Y.E.; Yates, C.J. A statistical explanation of MaxEnt for ecologists. *Divers. Distrib.* **2011**, *17*, 43–57. [CrossRef]

46. Arzoumanian, Z.; Holmberg, J.; Norman, B. An astronomical pattern-matching algorithm for computer-aided identification of whale sharks *Rhincodon typus*. *J. Appl. Ecol.* **2005**, *42*, 999–1011. [CrossRef]
47. Brooks, K.; Rowat, D.; Pierce, S.J.; Jouannet, D.; Vely, M.A. Seeing spots: Photo-identification as a regional tool for whale shark identification. *WIO J. Mar. Sci.* **2010**, *9*, 185–194.
48. McCoy, E.; Burce, R.; David, D.; Aca, E.Q.; Hardy, J.; Labaja, J.; Snow, S.J.; Ponzo, A.; Araujo, G. Long-term photo-identification reveals the population dynamics and strong site fidelity of adult whale sharks to the coastal waters of Donsol, Philippines. *Front. Mar. Sci.* **2018**, *5*, 271. [CrossRef]
49. Matsumoto, R.; Toda, M.; Matsumoto, Y.; Ueda, K.; Nakazato, M.; Sato, K.; Uchida, S. Notes on Husbandry of Whale Sharks, *Rhincodon typus*, in Aquaria. In *The Elasmobranch Husbandry Manual II: Recent Advances in the Care of Sharks, Rays and Their Relatives*, 1st ed.; Smith, M., Warmolts, D., Thoney, D., Hueter, R., Murray, M., Ezcurra, J., Eds.; Ohio Biological Survey, Inc.: Columbus, OH, USA, 2017; pp. 15–22.
50. Rees, G. *Physical Principles of Remote Sensing*, 3rd ed.; Cambridge University Press: Cambridge, UK, 2013; pp. 67–70.
51. Rohner, C.A.; Prebble, C.E.M. Whale Shark Foraging, Feeding, and Diet. In *Whale Sharks Biology, Ecology, and Conservation*, 1st ed.; Rohner, C.A., Prebble, C.E.M., Eds.; CRC Press: Boca Raton, FL, USA, 2021; pp. 153–180. [CrossRef]
52. Rowat, D.R.; Leblond, S.T.; Pardigon, B.; Vely, M.A.; Jouannet, D.; Webster, I.A. Djibouti-a kindergarten for whale sharks? Qscience. In Proceedings of the 4th International Whale Shark Conference, Doha, Qatar, 16–18 May 2016. [CrossRef]
53. Simpfendorfer, C.A.; Heupel, M.R.; White, W.T.; Dulvy, N.K. The Importance of Research and Public Opinion to Conservation Management of Sharks and Rays: A Synthesis. *Mar. Freshw. Res.* **2011**, *62*, 518–527. [CrossRef]
54. Robbins, R.L.; Booth, D.J. Seasonal, sexual and size segregation of White sharks, *Carcharodon carcharias*, at the Neptune Islands, South Australia. In *Global Perspectives on the Biology and Life History of the White Shark*; Domeier, M.L., Ed.; CRC Press: Boca Raton, FL, USA, 2012; pp. 225–254. [CrossRef]
55. Jacoby, D.M.P.; Busawon, D.S.; Sims, D.W. Sex and social networking: The influence of male presence on social structure of female shark groups. *Behav. Ecol.* **2010**, *21*, 808–818. [CrossRef]
56. Maxwell, S.M.; Scales, K.L.; Bograd, S.J.; Briscoe, D.K.; Dewar, H.; Hazen, E.L.; Lewison, R.L.; Welch, H.; Crowder, L.B. Seasonal spatial segregation in blue sharks (*Prionace glauca*) by sex and size class in the Northeast Pacific Ocean. *Divers. Distrib.* **2019**, *25*, 1304–1317. [CrossRef]
57. Meekan, M.G.; Taylor, B.M.; Lester, E.; Ferreira, L.C.; Sequeira, A.M.M.; Dove, A.D.M.; Birt, M.J.; Aspinall, A.; Brooks, K.; Thums, M. Asymptotic Growth of Whale Sharks Suggests Sex-Specific Life-History Strategies. *Front. Mar. Sci.* **2020**, *7*, 575683. [CrossRef]
58. Prebble, C.E.M.; Rohner, C.A.; Pierce, S.J.; Robinson, D.P.; Jaidah, M.Y.; Bach, S.S.; Trueman, C.N. Limited latitudinal ranging of juvenile whale sharks in the Western Indian Ocean suggests the existence of regional management units. *Mar. Ecol. Prog. Ser.* **2018**, *601*, 167–183. [CrossRef]
59. Rohner, C.A.; Cochran, J.E.M.; Cagua, E.F.; Prebble, C.E.M.; Venables, S.K.; Berumen, M.L.; Kuguru, B.L.; Rubens, J.; Brunnschweiler, J.M.; Pierce, S.J. No Place Like Home? High Residency and Predictable Seasonal Movement of Whale Sharks Off Tanzania. *Front. Mar. Sci.* **2020**, *7*, 423. [CrossRef]
60. Rohner, C.A.; Norman, B.; Reynolds, S.; Araujo, G.; Holmberg, J.; Pierce, S.J. Population Ecology of Whale Sharks. In *Whale Sharks*, 1st ed.; Rohner, C.A., Prebble, C.E.M., Eds.; CRC Press: Boca Raton, FL, USA, 2021; pp. 129–152. [CrossRef]
61. Heyman, W.D.; Graham, R.T.; Kjerfve, B.; Johannes, R.E. Whale sharks *Rhincodon typus* aggregate to feed on fish spawn in Belize. *Mar. Ecol. Prog. Ser.* **2001**, *215*, 275–282. [CrossRef]
62. de la Parra Venegas, R.; Hueter, R.; Cano, J.G.; Tyminski, J.; Remolina, J.G.; Maslanka, M.; Ormos, A.; Weigt, L.; Carlson, B.; Dove, A. An unprecedented aggregation of whale sharks, *Rhincodon typus*, in Mexican coastal waters of the Caribbean Sea. *PLoS ONE* **2011**, *6*, e18994. [CrossRef]
63. Hacohen-Domené, A.; Martínez-Rincón, R.O.; Galván-Magaña, F.; Cárdenas-Palomo, N.; de la Parra-Venegas, R.; Galván Pastoriza, B.; Dove, A.D.M. Habitat suitability and environmental factors affecting whale shark (*Rhincodon typus*) aggregations in the Mexican Caribbean. *Environ. Biol. Fishes* **2015**, *98*, 1953–1964. [CrossRef]
64. Friedlaender, A.S.; Halpin, P.N.; Qian, S.S.; Lawson, G.L.; Wiebe, P.H.; Thiele, D.; Read, A.J. Whale distribution in relation to prey abundance and oceanographic processes in shelf waters of the Western Antarctic Peninsula. *Mar. Ecol. Prog. Ser.* **2006**, *317*, 297–310. [CrossRef]
65. McKinney, J.; Hoffmayer, E.R.; Wu, W.; Fulford, R.; Hendon, J.M. Feeding habitat of the whale shark *Rhincodon typus* in the northern Gulf of Mexico determined using species distribution modelling. *Mar. Ecol. Prog. Ser.* **2012**, *458*, 199–211. [CrossRef]
66. Robinson, D.P.; Jaidah, M.Y.; Jabado, R.W.; Lee-Brooks, K.; El-Din, N.M.N.; Malki, A.A.A.; Elmeer, K.; McCormick, P.A.; Henderson, A.C.; Pierce, S.J.; et al. Whale sharks, *Rhincodon typus*, aggregate around Offshore Platforms in Qatari waters of the Arabian Gulf to feed on Fish Spawn. *PLoS ONE* **2013**, *8*, e58255. [CrossRef]
67. Cárdenas-Palomo, N.; Herrera-Silveira, J.; Velázquez-Abunader, I.; Reyes, O.; Ordoñez, U. Distribution and feeding habitat characterization of whale shark (*Rhincodon typus*) in a protected area in the Caribbean Sea. *J. Fish. Biol.* **2015**, *86*, 668–686. [CrossRef]

68. Eckert, S.A.; Stewart, B.S. Telemetry and Satellite Tracking of Whale Sharks, *Rhincodon typus*, in the Sea of Cortez, Mexico, and the North Pacific Ocean. *Environ. Biol. Fishes* **2001**, *60*, 299–308. [CrossRef]
69. Rowat, D.; Engelhardt, U. Seychelles: A case study of community involvement in the development of whale shark ecotourism and its socio-economic impact. *Fisheries Res.* **2007**, *84*, 109–113. [CrossRef]
70. Nakamura, I.; Matsumoto, R.; Sato, K. Body temperature stability in the whale shark, the world's largest fish. *J. Exp. Biol.* **2020**, *223*, 210286. [CrossRef]
71. Rohner, C.A.; Couturier, L.I.E.; Richardson, A.J.; Pierce, S.J.; Prebble, C.E.M.; Gibbons, M.J.; Nichols, P.D. Diet of Whale Sharks *Rhincodon Typus* Inferred from Stomach Content and Signature Fatty Acid Analyses. *Mar. Ecol. Prog. Ser.* **2013**, *493*, 219–235. [CrossRef]
72. Robinson, D.P.; Jaidah, M.Y.; Bach, S.S.; Lee, K.; Jabado, R.W.; Rohner, C.A.; March, A.; Caprodossi, S.; Henderson, A.C.; Mair, J.M.; et al. Population Structure, Abundance and Movement of Whale Sharks in the Arabian Gulf and the Gulf of Oman. *PLoS ONE* **2016**, *11*, e0158593. [CrossRef]
73. Nelson, J.D.; Eckert, S.A. Foraging ecology of whale sharks (*Rhincodon typus*) within Bahía de Los Angeles, Baja California Norte, México. *Fish. Res.* **2007**, *84*, 47–64. [CrossRef]
74. Almogi-Labin, A.; Schmiedl, G.; Hemleben, C.; Siman-Tov, R.; Segl, M.; Meischner, D. The influence of the NE winter monsoon on productivity changes in the Gulf of Aden, NW Arabian Sea, during the last 530 ka as recorded by benthic foraminifera. *Mar. Micropaleontol.* **2000**, *40*, 295–319. [CrossRef]
75. Graham, W.M.; Largier, J.L. Upwelling shadows as nearshore retention sites: The example of northern Monterey Bay. *Cont. Shelf Res.* **1997**, *17*, 509–532. [CrossRef]
76. Castelão, R.M.; Mavor, T.P.; Barth, J.A.; Breaker, L.C. Sea surface temperature fronts in the California Current System from geostationary satellite observations. *J. Geophys. Res.* **2006**, *111*, C09026. [CrossRef]
77. Woodson, C.B.; McManus, M.A.; Tyburczy, J.A.; Barth, J.A.; Washburn, L.; Caselle, J.E.; Carr, M.H.; Malone, D.P.; Raimondi, P.T.; Menge, B.A.; et al. Coastal Fronts Set Recruitment and Connectivity Patterns across Multiple Taxa. *Limnol. Oceanogr.* **2012**, *57*, 582–596. [CrossRef]
78. Escribano, R.; Hidalgo, P.; Valdés, V.; Frederick, L. Temperature effects on development and reproduction of copepods in the Humboldt Current: The advantage of rapid growth. *J. Plankton Res.* **2014**, *36*, 104–116. [CrossRef]
79. D'Antonio, B.; Ferreira, L.C.; Meekan, M.; Thomson, P.G.; Lieber, L.; Virtue, P.; Power, C.; Pattiaratchi, C.B.; Brierley, A.S.; Sequeira, A.M.M.; et al. Links between the three-dimensional movements of whale sharks (*Rhincodon typus*) and the bio-physical environment off a coral reef. *Mov. Ecol.* **2024**, *12*, 10. [CrossRef] [PubMed]
80. Hanson, C.E.; Pattiaratchi, C.B.; Waite, A.M. Sporadic upwelling on a downwelling coast: Phytoplankton responses to spatially variable nutrient dynamics off the Gascoyne region of Western Australia. *Cont. Shelf Res.* **2005**, *25*, 1561–1582. [CrossRef]
81. Woo, M.; Pattiaratchi, C.; Schroeder, W. Dynamics of the Ningaloo current off Point Cloates, Western Australia. *Mar. Freshw. Res.* **2006**, *57*, 291–301. [CrossRef]
82. Rousseaux, C.S.G.; Lowe, R.; Feng, M.; Waite, A.M.; Thompson, P.A. The role of the Leeuwin Current and mixed layer depth on the autumn phytoplankton bloom off Ningaloo Reef, Western Australia. *Cont. Shelf Res.* **2012**, *32*, 22–35. [CrossRef]
83. Marcus, L.; Virtue, P.; Pethybridge, H.R.; Meekan, M.G.; Thums, M.; Nichols, P.D. Intraspecific Variability in Diet and Implied Foraging Ranges of Whale Sharks at Ningaloo Reef, Western Australia, from Signature Fatty Acid Analysis. *Mar. Ecol. Prog. Ser.* **2016**, *554*, 115–128. [CrossRef]
84. Macena, B.C.L.; Hazin, F.H.V. Whale shark (*Rhincodon typus*) seasonal occurrence, abundance and demographic structure in the Mid-Equatorial Atlantic Ocean. *PLoS ONE* **2016**, *11*, e0164440. [CrossRef]
85. Omar, Y.M.; Memery, L.; Carton, X.; Daher, A.; Duvielbourg, E. Effects of Monsoon Winds and Topographical Features on the Vertical Thermohaline and Biogeochemical Structure in the Gulf of Tadjoura (Djibouti). *Open J. Mar. Sci.* **2016**, *6*, 440–455. [CrossRef]